

Cell Reports Medicine, Volume 5

Supplemental information

Gemcitabine therapeutically disrupts essential

SIRT1-mediated p53 repression in atypical

teratoid/rhabdoid tumors

Dennis S. Metselaar, Michaël H. Meel, Joshua R. Goulding, Aimeé du Chatinier, Leyla Rigamonti, Piotr Waranecki, Neal Geisemeyer, Mark C. de Gooijer, Marjolein Breur, Jan Koster, Sophie E.M. Veldhuijzen van Zanten, Marianna Bugiani, Niels E. Franke, Alyssa Reddy, Pieter Wesseling, Gertjan J.L. Kaspers, and Esther Hulleman

Supplementary figures

Brain tumor methylation classifier results (v11b4)

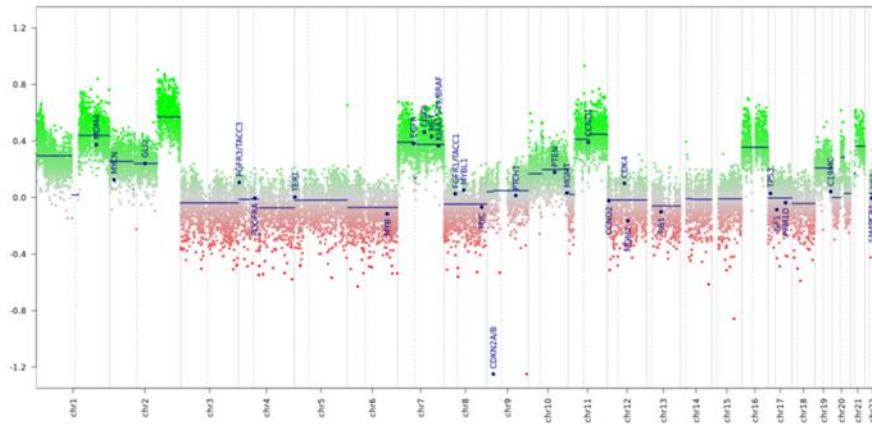
| Methylation classes (MCs with score ≥ 0.3) | Calibrated score | Interpretation | |
|--|------------------|----------------|---|
| methylation class family Atypical teratoid/rhabdoid tumor | 0.96 | match | ✓ |
| MC family members with score ≥ 0.1 | | | |
| methylation class atypical teratoid/rhabdoid tumor, subclass SHH | 0.95 | match | ● |

Legend: ✓ Match (score ≥ 0.9) ✗ No match (score < 0.9): possibly still relevant for low tumor content and low DNA quality cases. ● Match to MC family member (score ≥ 0.5)

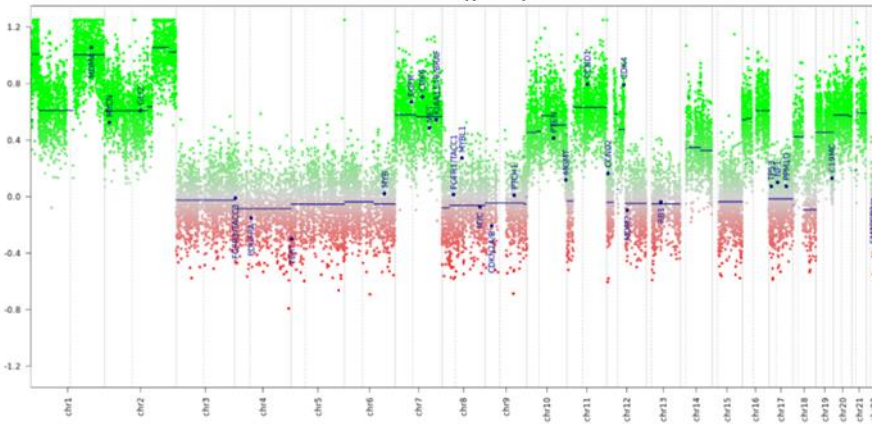
Supplementary figure S1: VUMC-ATRT-03 resected tumor tissue classifies as SHH subtype ATRT, related to Figure 1.

Methylome profiling analysis of the VUMC-ATRT-03 cells and matching of this profile with the Heidelberg Brain Tumors Classifier⁴⁴ (PMID 29539639; www.moleculareuropathology.org) confirms that these cells belong to the SHH subgroup of ATRT.

CNV: VUMC-ATRT-03 tumor tissue

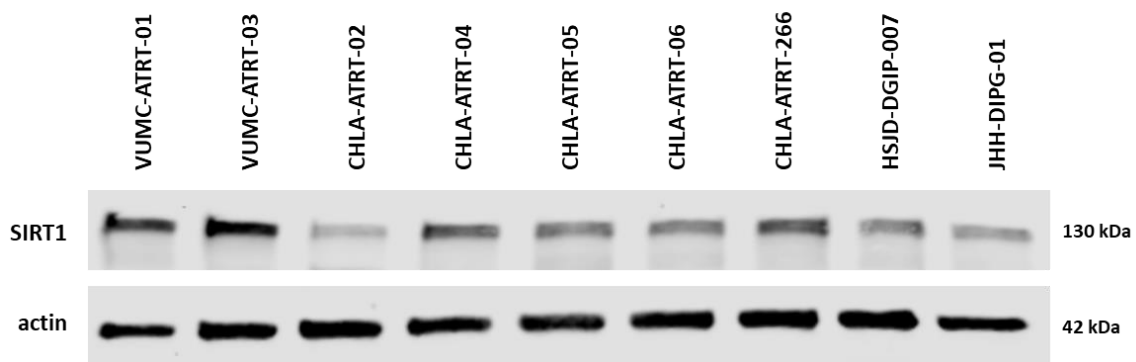


CNV: VUMC-ATRT-03 cell culture (p10)



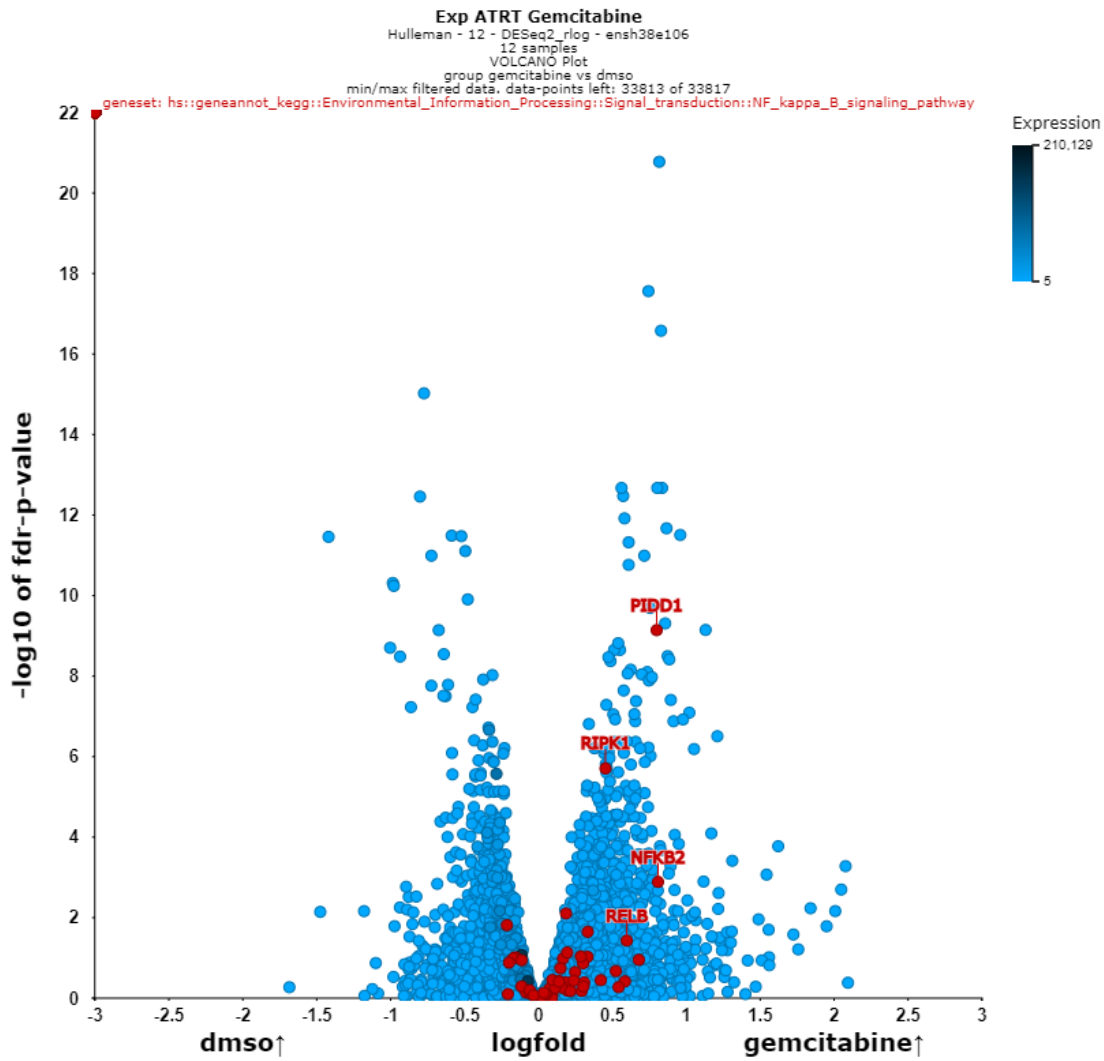
Supplementary figure S2: Copy number profile is maintained between tumor tissue and cell culture, related to Figure 1.

Genomic copy number variation profile of VUMC-ATRT-03 patient-derived tumor tissue (upper panel) and VUMC-ATRT-03 mouse passage cells (lower panel).



Supplementary figure S3: SIRT1 baseline expression in culture models, related to Figure 3.

Western blot analysis depicting SIRT1 baseline expression in seven ATRT cell cultures and two DMG cell cultures as non-ATRT control.

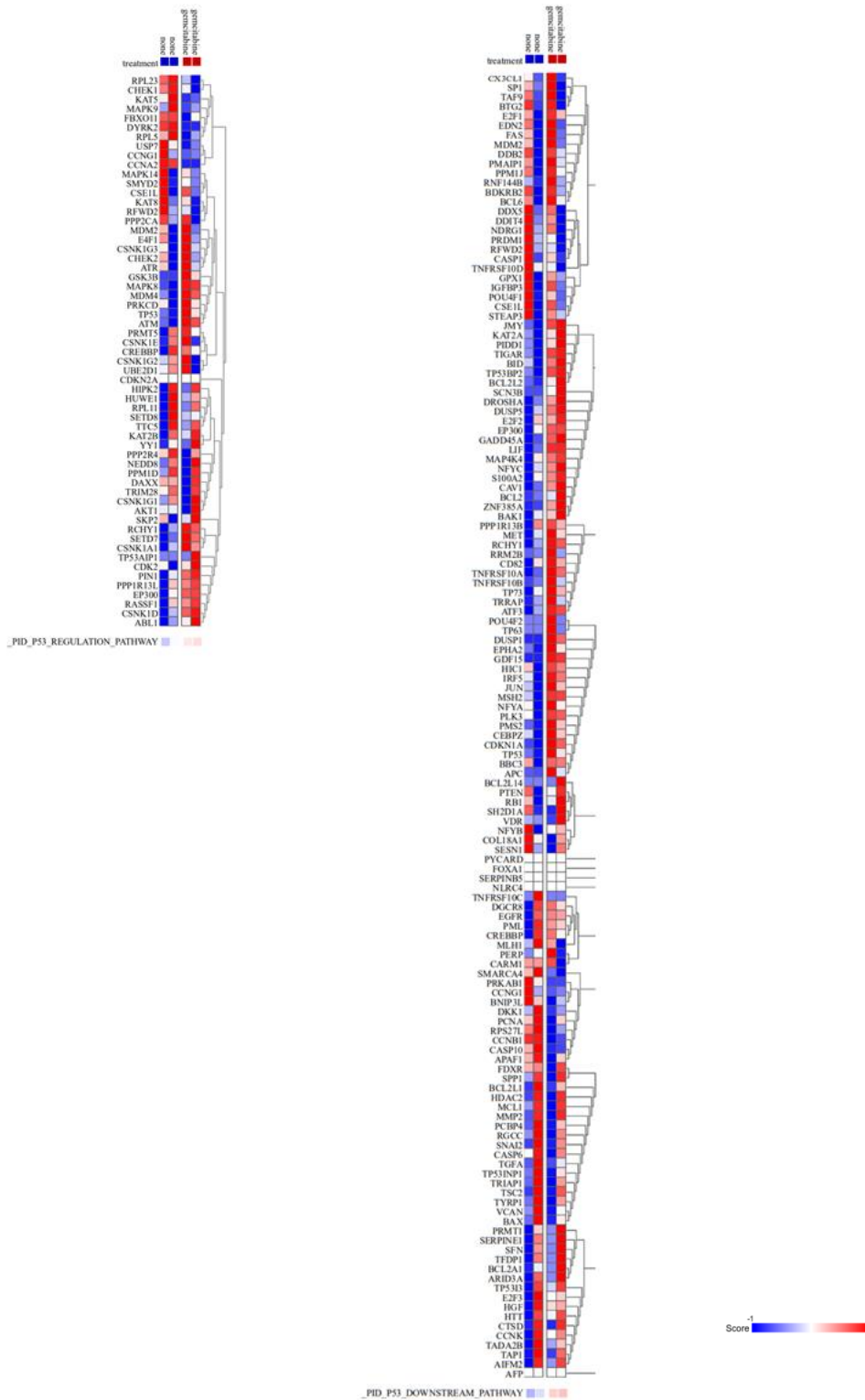


Supplementary figure S4: Gemcitabine upregulates NF-κB pathway, related to Figure 3.

Vulcano plot depicting $-\log_{10}$ fdr-corrected p-value of differential expressed genes between DMSO (n=6) and gemcitabine treated (n=6) ATRT cell cultures VUMC-ATRT-01, VUMC-ATRT-03, CHLA-02, CHLA-05, CHLA-06, and CHLA-266. All 92 genes of the ‘KEGG NF-kappa_B_signaling_pathway’ are highlighted in red.

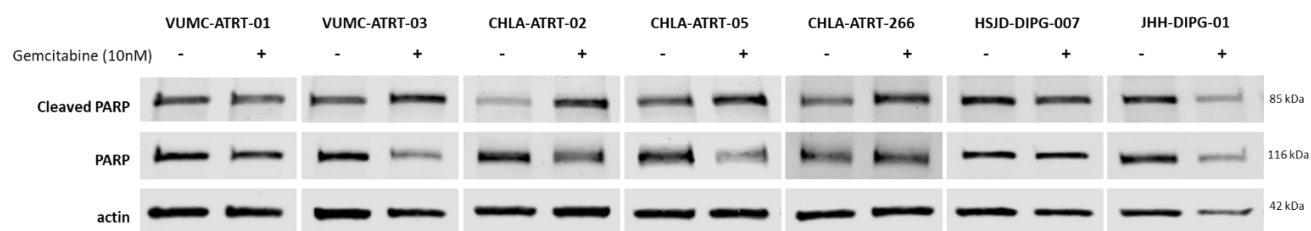
p53 upstream regulators

p53 downstream targets



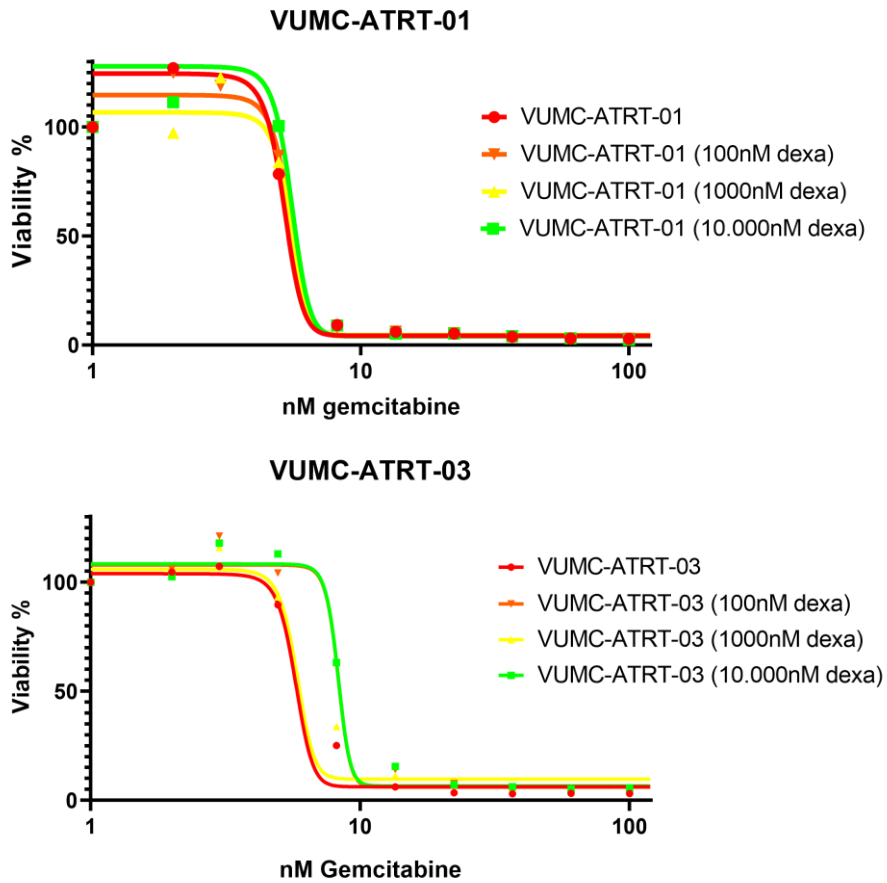
Supplementary figure S5: p53 upstream and downstream regulators are upregulated by gemcitabine treatment, related to Figure 3.

Heatmap representation illustrating mRNA expression of the Broad Institute curated database p53 upstream regulating genes (left) and p53 downstream target genes (right) from RNA-sequencing data showing non-treated versus gemcitabine treated VUMC-ATRT-01 and VUMC-ATRT-03 cultures. Average expression of the full gene set is depicted at the bottom of both heatmaps.



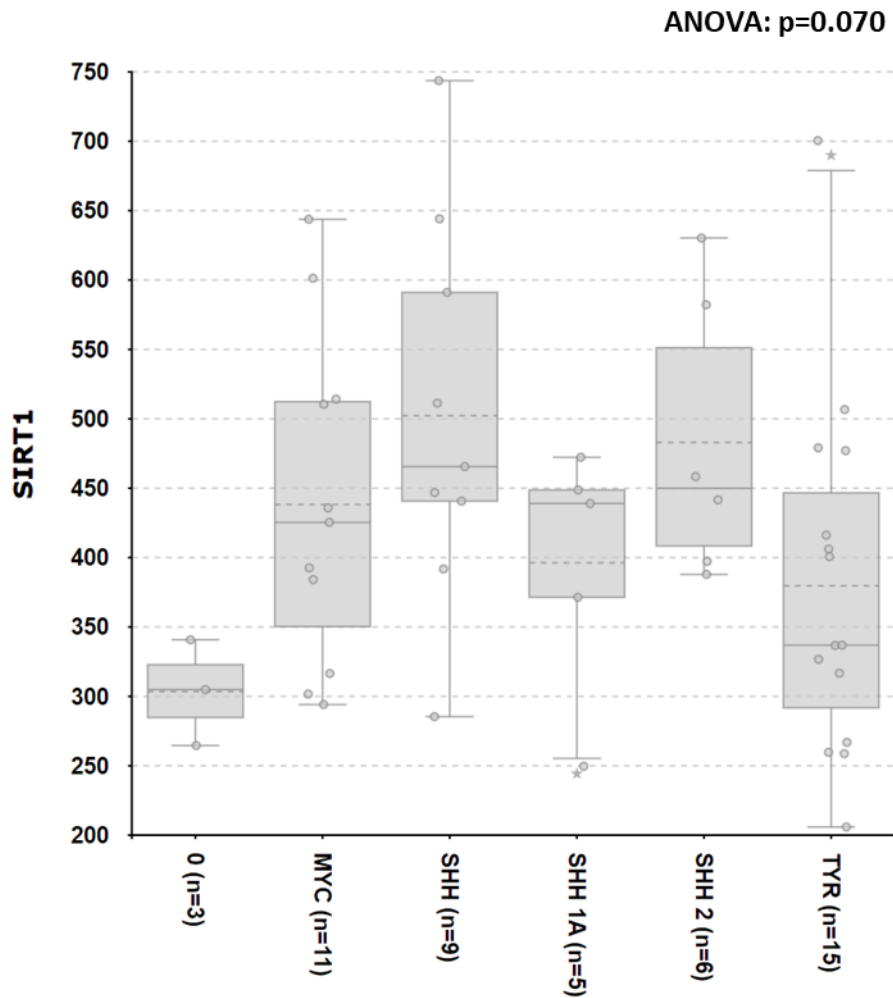
Supplementary figure S6: Gemcitabine treatment induces apoptosis in ATRT cells, related to Figure 3.

Western blot analysis depicting cleaved-PARP and PARP in five ATRT cell cultures and two DMG cell cultures as non-ATRT control. Except VUMC-ATRT-01 the other four ATRT models show a visible increase in cleaved-PARP while both DMG cultures do not.



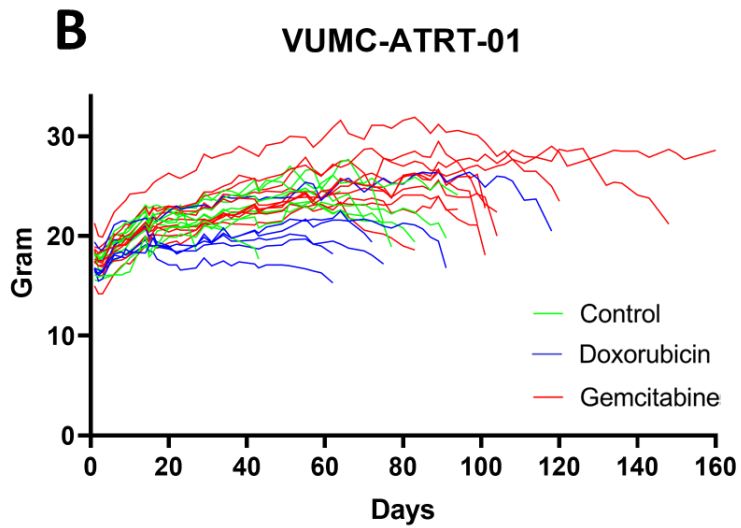
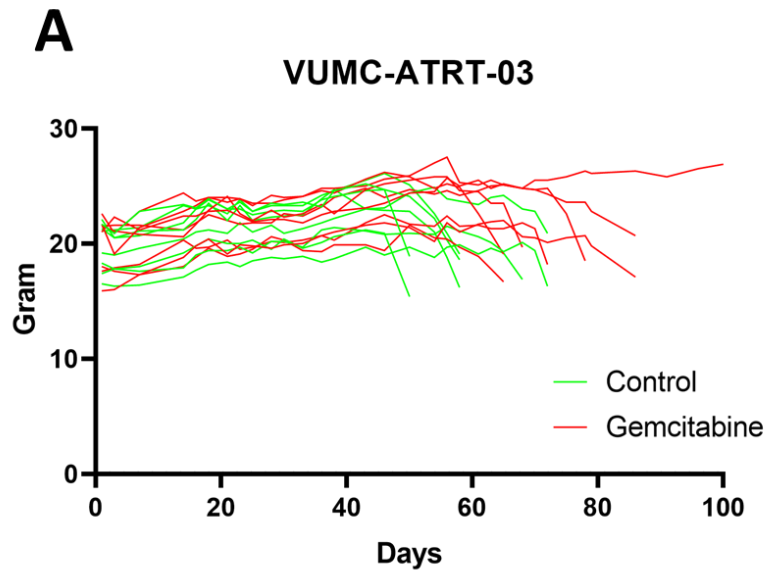
Supplementary figure S7: Dexamethasone treatment does not decrease gemcitabine treatment efficacy, related to Figure 3.

IC50 viability curves of gemcitabine treatment combined with a dexamethasone concentration in VUMC-ATR1-01 and VUMC-ATR1-03 cells treated for 96h.



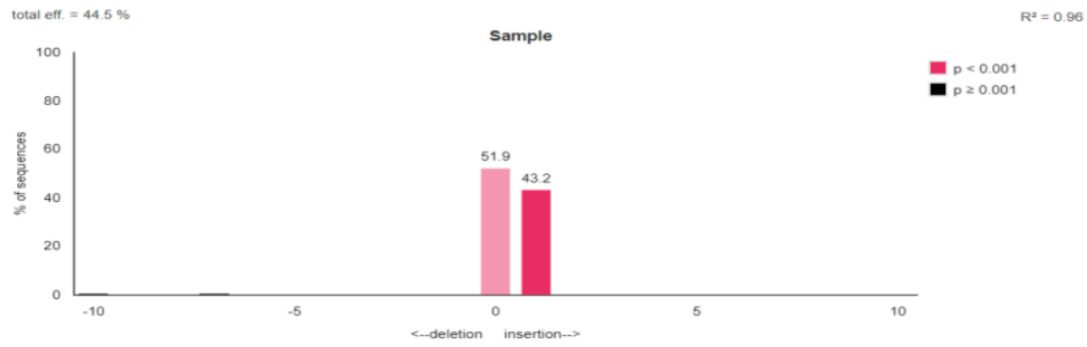
Supplementary figure S8: SIRT1 expression is not specific to any ATRT subtypes, related to Figure 5.

Box plot graph depicting SIRT1 mRNA expression in the 49 ATRT tissue samples from the Kool dataset (GSE: 70678) subdivided into the currently described subgroups. Subgroup annotation was achieved through re-clustering of methylation data of each of the samples. However, three samples could not be annotated to any subgroup and nine samples could only be annotated to the SHH cluster, without further subclassification. No significant differences between groups are observed (two-way ANOVA: p=0.070).

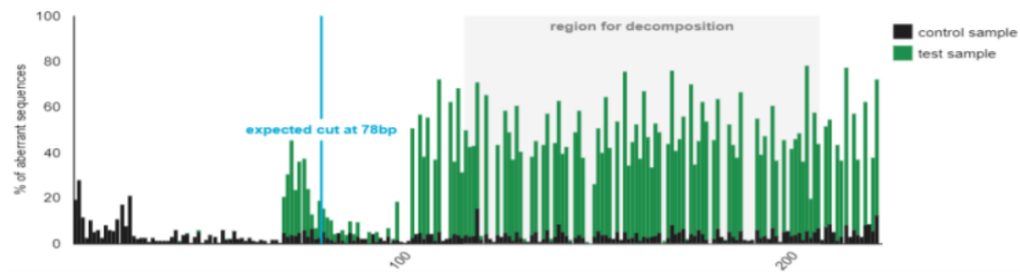


Supplementary figure S9: Gemcitabine treatment did not cause *in vivo* toxicity, related to Figure 6.

(A) Weight development of VUMC-ATRTR-03 orthotopic xenograft bearing mice over time (control in green, gemcitabine treated in red). (B) Weight development of VUMC-ATRTR-01 orthotopic xenograft bearing mice over time (control in green, doxorubicin treated in blue, gemcitabine treated in red).



Quality control - Aberrant sequence signal



Supplementary figure S10: TP53 indel efficiency in VUMC-ATRT-03 cells upon Cas9 and TP53 sgRNA transduction, related to START Methods.

Upper panel: decomposition yielding the spectrum of indels and their frequencies (before blasticidin selection) as analyzed by TIDE. Lower panel: visualization of aberrant sequence signal in control (black) and treated sample (green). The region used for decomposition is indicated with a gray bar; the expected break site with a vertical blue line.

Supplementary Tables

| Compounds tested at 1000nM | IC50 <1000nM for VUMC-ATRT-03 | IC50 <1000nM for tested DMG cultures (average) |
|----------------------------------|-------------------------------|--|
| <i>Panobinostat</i> | Panobinostat | Panobinostat |
| <i>LAQ824</i> | LAQ824 | LAQ824 |
| <i>Chaetocin</i> | Chaetocin | Chaetocin |
| <i>HC Toxin</i> | HC Toxin | HC Toxin |
| <i>CUDC-101</i> | CUDC-101 | CUDC-101 |
| <i>Apicidin</i> | Apicidin | Apicidin |
| <i>ITF-2357</i> | SB939 | ITF-2357 |
| <i>MI-2 (hydrochloride)</i> | Trichostatin A | MI-2 (hydrochloride) |
| <i>SB939</i> | Gemcitabine | SB939 |
| <i>Trichostatin A</i> | 4-iodo-SAHA | Trichostatin A |
| <i>Gemcitabine</i> | CAY10603 | MS-275 |
| <i>MS-275</i> | JIB-04 | 4-iodo-SAHA |
| <i>4-iodo-SAHA</i> | GSK-J4 (hydrochloride) | CAY10398 |
| <i>CAY10398</i> | Tubacin | Chidamide |
| <i>Chidamide</i> | | SAHA |
| <i>SAHA</i> | | Etoposide |
| <i>Etoposide</i> | | Scriptaid |
| <i>Scriptaid</i> | | M 344 |
| <i>M 344</i> | | Lestaurtinib |
| <i>Lestaurtinib</i> | | OTX015 |
| <i>OTX015</i> | | (+)-JQ1 |
| <i>(+)-JQ1</i> | | Bromosporine |
| <i>Bromosporine</i> | | Decitabine |
| <i>Decitabine</i> | | CPI-203 |
| <i>CPI-203</i> | | CAY10603 |
| <i>CAY10603</i> | | I-BET151 |
| <i>I-BET151</i> | | Oxaflatin |
| <i>Oxaflatin</i> | | 6-Thioguanine |
| <i>6-Thioguanine</i> | | |
| <i>Coumarin-SAHA</i> | | |
| <i>Tenovin-1</i> | | |
| <i>(-)-Neplanocin A</i> | | |
| <i>I-BET762</i> | | |
| <i>Pyroxamide</i> | | |
| <i>3-Deazaneplanocin A</i> | | |
| <i>3-Deazaneplanocin A</i> | | |
| <i>CI-994</i> | | |
| <i>AK-7</i> | | |
| <i>Rucaparib (phosphate)</i> | | |
| <i>CBHA</i> | | |
| <i>Pimelic Diphenylamide 106</i> | | |
| <i>5-Azacytidine</i> | | |
| <i>GSK126</i> | | |
| <i>UNC0631</i> | | |
| <i>PFI-1</i> | | |
| <i>SGC0946</i> | | |
| <i>UNC1999</i> | | |
| <i>CPTH2 (hydrochloride)</i> | | |
| <i>JIB-04</i> | | |
| <i>BIX01294</i> | | |
| <i>Delphinin (chloride)</i> | | |
| <i>CAY10591</i> | | |
| <i>Garcinol</i> | | |
| <i>EPZ5676</i> | | |
| <i>CCG-100602</i> | | |
| <i>UNC0646</i> | | |
| <i>HPOB</i> | | |
| <i>Sinefungin</i> | | |
| <i>GSK343</i> | | |
| <i>CAY10433</i> | | |
| <i>UNC0638</i> | | |
| <i>Anacardic Acid</i> | | |
| <i>Salermide</i> | | |
| <i>CAY10683</i> | | |
| <i>AGK7</i> | | |
| <i>UNC0642</i> | | |
| <i>GSK-J4 (hydrochloride)</i> | | |
| <i>GSK-J2 (sodium salt)</i> | | |
| <i>Phthalazinone pyrazole</i> | | |
| <i>Piceatannol</i> | | |
| <i>Nullscript</i> | | |
| <i>5-Methylcytidine</i> | | |
| <i>1-Naphthoic Acid</i> | | |
| <i>JGB1741</i> | | |
| <i>EPZ005687</i> | | |
| <i>RSC-133</i> | | |
| <i>5-Methyl-2'-deoxycytidine</i> | | |
| <i>Sirtinol</i> | | |

| | | |
|---|--|--|
| <p><i>Zebularine</i> <i>2-hexyl-4-Pentynoic Acid</i> <i>CAY10669</i> <i>Sodium Butyrate</i> <i>GSK4112</i> <i>AMI-1 (sodium salt)</i> <i>Tubastatin A</i> <i>S-(5'-Adenosyl)-L-methionine</i> <i>Daminozide</i> <i>AZ 505</i> <i>Sodium 4-Phenylbutyrate</i> <i>Mirin</i> <i>I-CBP112 (hydrochloride)</i> <i>C646</i> <i>Ellagic Acid</i> <i>Suberohydroxamic Acid</i> <i>GSK-LSD1 (hydrochloride)</i> <i>GSK-J5 (hydrochloride)</i> <i>UNC1215</i> <i>Cl-Amidine</i> <i>RGFP966</i> <i>Valproic Acid (sodium salt)</i> <i>F-Amidine</i> <i>IOX1</i> <i>(+)-Abscisic Acid</i> <i>(-)-JQ1</i> <i>Suramin (sodium salt)</i> <i>MI-nc (hydrochloride)</i> <i>B32B3</i> <i>Isoliquiritigenin</i> <i>SAHA-Bpyne</i> <i>Acetyl-a-ketoglutarate</i> <i>AGK2</i> <i>RVX-208</i> <i>2,4-DPD</i> <i>DMOG</i> <i>GSK-J1 (sodium salt)</i> <i>UNC0321</i> <i>Splitomicin</i> <i>3,3'-Diindolylmethane</i> <i>Nicotinamide</i> <i>Tubacin</i> <i>2-PCPA (hydrochloride)</i> <i>a-Hydroxyglutaric Acid</i> <i>Butyrolactone 3</i> <i>WDR5-0103</i> <i>SIRT1/2 inhibitor IV</i> <i>2',3',5'-triacetyl-5-</i> <i>Azacytidine</i> <i>Tubastatin A</i> <i>UNC0224</i> <i>EX-527</i> <i>MS-436</i> <i>S-Adenosylhomocysteine</i> <i>RG-108</i> <i>SGC-CBP30</i> <i>PCI 34051</i> <i>2,4-Pyridinedicarboxylic Acid</i> <i>S-(5'-Adenosyl)-L-methionine</i> <i>chloride</i> <i>BRD73954</i> <i>HNHA</i> <i>trans-Resveratrol</i> <i>N-Oxalylglycine</i> <i>3-amino Benzamide</i> <i>BSI-201</i> <i>Lomeguatrib</i> <i>SGI-1027</i> <i>4-pentynoyl-Coenzyme A</i> <i>MC 1568</i></p> | | |
|---|--|--|

Supplementary table S1: related to Figure 2.

Additional information to the drug screening results of figure 2A. Left column lists all tested compounds. Middle column lists compounds with viability score below 50% at 1000nM for VUMC-ATRT-03 cells. Right column lists compounds with (average) viability score below 50% at 1000nM for VUMC-DIPG-10, VUMC-DIPG-11, VUMC-DIPG-F, JHH-DIPG-01, VUMC-DIPG-A, VUMC-HGG-09, SU-pcGBM-02, KNS-42, and HSJD-DIPG-07.

| Geneset | Gemcitabine > None |
|--|--------------------|
| REACTOME_HEDGEHOG_OFF_STATE (113) | -6.115 |
| REACTOME_SIGNALING_BY_HEDGEHOG (150) | -5.750 |
| REACTOME_HEDGEHOG_ON_STATE (86) | -4.574 |
| REACTOME_HEDGEHOG_LIGAND_BIOGENESIS (65) | -4.552 |
| PID_HEDGEHOG_GLI_PATHWAY (48) | -3.118 |
| <i>Significance</i> | < -2.580 |

Supplementary table S2: Related to Figure 5.

Parametric assessment of geneset enrichment (PAGE) of VUMC-ATRT-03, VUMC-DIPG-10, VUMC-DIPG-11, VUMC-HGG-09, JHH-DIPG-01, HSJD-DIPG-07, and SU-pcGBM-2 cells after gemcitabine treatment (5nM, 24h), compared to non-treated conditions. All major Reactome (<https://reactome.org/>) and Pathway Interaction Database (PID) (<http://pid.nci.nih.gov/>) SHH-signaling pathways are shown significantly downregulated in gemcitabine treated conditions. Scores <-2.580 are statistically significant (FDR, p<0.05) (<http://r2.amc.nl/>).

| shRNA | Full Hairpin Sequence | Sense Sequence | Vector |
|------------|--|---------------------------|------------|
| shSIRT1 #1 | CCGGGCAAAGCCTTCTGAATCTATCTCGAG ATAGATTGAGAAAGGCTTTGCTTTTT | GCAAAGCCTTTCTGAAT CTAT | pLKO. 1 |
| shSIRT1 #2 | CCGGCCTCGAACAATCTTAAAGATCTCGAG ATCTTTAAGAATTGTTGAGGTTTT | CCTCGAACAATTCTTAA AGAT | pLKO. 1 |
| shSIRT1 #3 | CCGGGCGGGAATCCAAAGGATAATCTCGAG AATTATCCTTTGGATTCCCGCTTTTT | GCGGGAATCCAAAGGAT AATT | pLKO. 1 |

Supplementary table S3: Related to STAR Methods.

shRNA sequences (sense in blue, antisense in red) of constructs used in this study.

| Primer | Sequence |
|-----------------------|--------------------------|
| TP53 exon4 FWD primer | caccGAAGGGACAGAAGATGACAG |
| TP53 exon4 REV primer | aaacCTGTCATCTTCTGTCCCTTC |
| hSpCas9 U6 Seq FWD | GAGGGCCTATTTCCCATGATTCC |

Supplementary table S4: Related to STAR Methods.

Relevant sequences for cloning p53 sgRNA into vector backbone, including sequencing primer for validation. Actual TP53 guide sequence is highlighted in blue.